Study of Local Minima in Metric Adaptive Optics

Justin D. Mansell[1], Aaron Masino, and Brian Henderson
Active Optical Systems, LLC, 2021 Girard Ste 150, Albuquerque, NM 87106

ABSTRACT

Metric adaptive optics systems search over a set of wavefront modes or commands to actuators to optimize a system performance metric like Strehl ratio or brightness. These systems have been explored for many decades and have been thought to be unreliable due to local minima in the metric space. It has been shown that some modes match well with no local minima to a given metric, but they rely on the ability of a mirror to create reliable replicas of the search modes. We present here a study of the most common implementation of metric adaptive optics that involves searching over the actuator command space while evaluating an intensity-based metric. We map an error space relating a common metric to actuator commands and statistically analyze the error function to determine the quantity and location of the local minima.

Keywords: Metric Adaptive Optics, Local Minima, Actuator Basis Set, Searching, Dithering, Target-in-the-Loop Adaptive Optics.

1. INTRODUCTION

In metric adaptive optics (MAO) aberrations on a beam of light are compensated by optimizing a metric of beam quality while searching through the commands sent to a deformable mirror. This technique is also known as Target-in-the-Loop Adaptive Optics or Stochastic Adaptive Optics. The most commonly used metric is the amount of light propagating to a focus through a pinhole onto a photodiode. Other metrics that have been considered include the amount of focused light propagating through a complicated intensity mask or the rms wavefront slopes measured on a wavefront sensor.

In contrast, conventional adaptive optics (CAO) compensates aberrations on a beam of light by measuring the wavefront distortion on a wavefront sensor and then using a control matrix and an integrating control loop to command deformable mirror. There are several challenges to using conventional adaptive optics. CAO requires a wavefront sensor, which is often expensive. To measure the wavefront using a Shack-Hartmann wavefront sensor, a curvature sensor, or phase diversity sensor, the beam of light needs to be spread-out over many pixels. Many applications of adaptive optics site photon flux as the fundamental limit of the bandwidth of the system. Finally, there is often a significant delay between the measurement on the wavefront sensor and the commands being sent to the deformable mirror due to the significant amount of processing required to convert the image into a phase measurement and then to convert the phase measurement into deformable mirror commands.

Metric adaptive optics offers solutions to many of these problems. The expensive complex wavefront sensor can be replaced with a low-cost high-speed photodiode. The complex computations can be replaced with a simple searching algorithm that can be implemented on a very low-cost microcontroller.[1]

There have been many different algorithms that have successfully demonstrated the optimization including stochastic parallel gradient descent (SPGD) and guided evolutionary simulated annealing (GESA).[2,3] These approaches usually search over the DM actuator commands to optimize the metric. Unfortunately, the error spaces generated by mapping the actuator commands to most of these metrics is well known to have local minima. A more deterministic approach involving searching through coefficients of Zernike-type polynomials was recently introduced to try to eliminate the local minima in this search space.[4] This algorithm relies on the ability to form the error space into a smooth local-minima free shape by warping the deformable mirror into these polynomial shapes. If the mirror cannot exactly match the polynomial shapes or there is noise on the detector, the error space is not guaranteed to be free of local-minima. Although

[1] jmansell@mza.com; phone 1 505 245-9970 x122

local minima are known to exist in the search space for MAO systems, they have not been well studied. We present here a study of one error space of a common implementation of metric adaptive optics. This study cannot address the limitations of all the possible variations of MAO systems, but will outline an analysis procedure that can be used for future studies of MAO search spaces. We begin with a description of how we setup the study and performed the analysis. Then we present results of statistical studies of two different error spaces.

2. ERROR SPACE GENERATION PROCEDURE

For this study, we chose to look at the ability for a 7 actuator deformable mirror to compensate an aberration generated as a sum of 10 Zernike polynomial terms using the integral form of Strehl ratio as the merit function.

The metric we used for this modeling was the integral form of the Strehl ratio (SR) given by,

$$SR = \frac{\left(\int\int E(x,y)\,dx\,dy\right)^2}{\int\int E(x,y)\cdot E(x,y)^*\,dx\,dy}$$

where E(x,y) is the field. A uniform intensity profile was used over the Zernike circle. This term was evaluated on a 32 by 32 grid with a grid spacing of 0.5625 mm.

The deformable mirror actuators were positioned in a hexagonal grid with a 4.5 mm spacing. The actuator influence functions were modeled as Gaussians with a $1/e^2$ radius of 6.1 mm. Figure 1 shows a cross-section of the influence function and a false-color plot of each of the influence functions on the grid used to for the merit function evaluation.

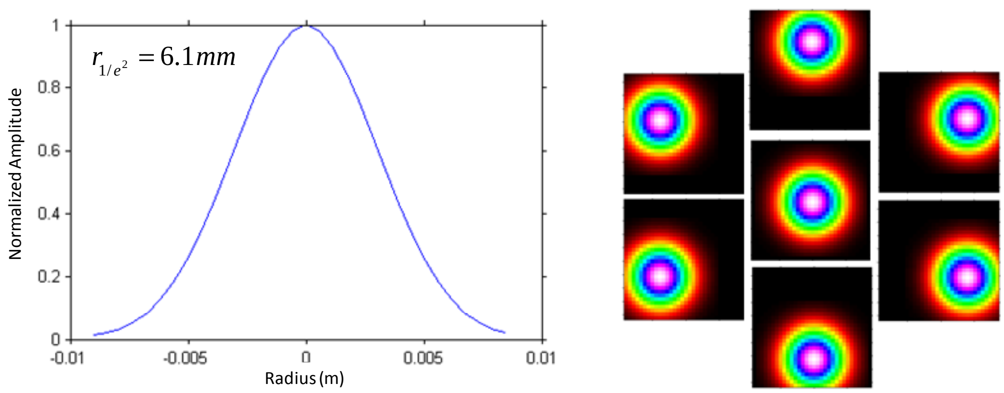

(a) (b)

Figure 1 - (a) is the cross-section of an individual influence function. (b) is the 2D false-color plot of each of the seven hexagonal-grid influence functions

The aberration was generated as a sum of the lowest-order 10 Zernike polynomial terms beyond piston using the Noll numbering. The common names of these Zernike terms are x tilt, y tilt, 90-degree astigmatism, focus, 45-degree astigmatism, x trefoil, x coma, y coma, y trefoil, and x quadrifoil. The Zernike coefficients were randomly generated using a Gaussian distribution with a sigma of π radians. The Zernike radius was set to 6.25 mm. Figure 3 shows false-color images of the three aberrations on the grid that was used to evaluate the merit function. Figure 2 shows the coefficients used in this modeling for the different aberrations that were evaluated.

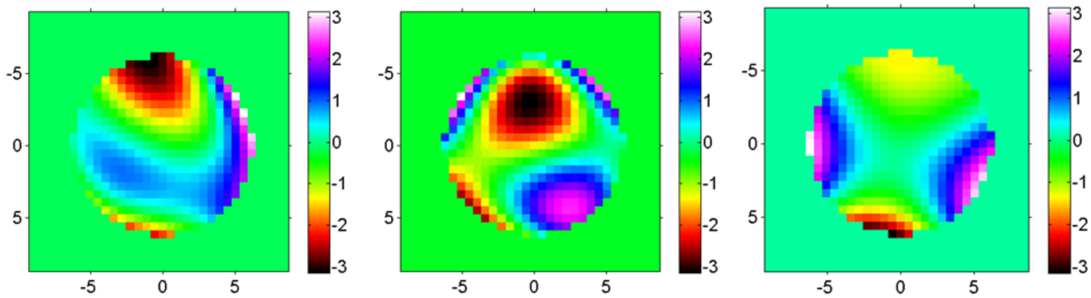

Figure 3 - False-color images of the three different aberrations evaluated.

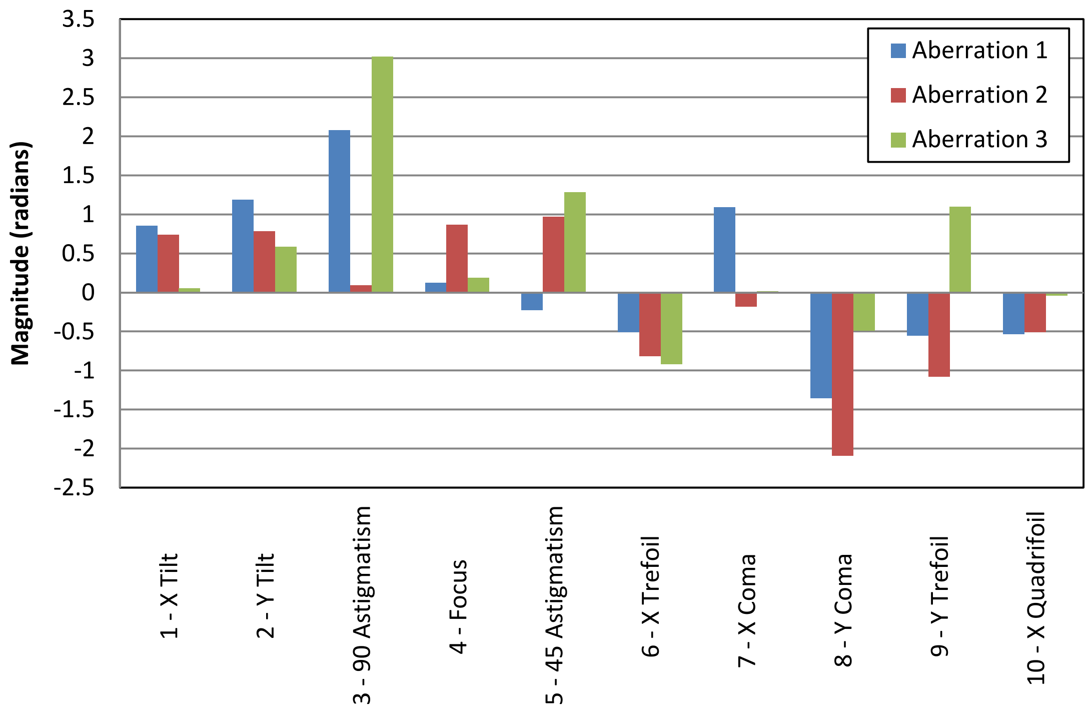

Figure 2 - Magnitude of the coefficients of the Zernike polynomial sum used to generate the aberration.

Once the aberration and the DM model were established, the error space around each of these aberrations was determined. We used a simple iterative axial searching algorithm to find the optimum position of the actuators to maximize the Strehl ratio. Then we evaluated the merit function at a regularly spaced 10 points between $-\pi$ and π around the optimum actuator positions for each actuator. Generation of the error space for a single aberration case involved the generation of 10^7 data points, which took about 4 days on a computer with a 2.4 GHz Intel Duo T7700 processor and 2 gigabytes of RAM. We limited ourselves to a noise-free error space for this study.

3. ERROR SPACE ANALYSIS

In this study, we studied the error space defined by the mapping of actuator positions to a Strehl ratio metric, which we generally want to maximize to get the best beam quality from a system. Therefore, we actually want to avoid local maxima, not local minima, but since the literature on this topic typically is trying to minimize an error, we will use the term local minima for consistency. In an operating system leveraging an existing search algorithm, we would probably negate the Strehl ratio to determine the error space, and would therefore create local minima instead of local maxima. After generating the error space we performed different types of analysis on the data to find the frequency, depth, order (number of local minima dimensions), and location of the local minima in this error space.

3.1. Frequency and Order of Local Minima

In a multi-dimensional error space it is possible for a point to be a minima in any number of dimensions. The first analysis we performed was to determine the frequency of the minima and in how many axes they were minima, which is referred to as the minima order or rank for this study. The global minimum is the point with the lowest error that is a minimum in all the axes. For this study, a point was considered a minima in an axis if the adjacent points in the error space along that axis were larger than it. Recall that the merit function was evaluated at 10 points between $-\pi$ and π around the optimum for each axis. Thus, each of the 7 axes has an edge at $-\pi$ and π, where it is not possible to evaluate the error function on both sides. Hence, it is not possible to determine if a point containing an edge is a local minima. Therfore, the analysis was done by ignoring the edges and looking at only the inner points of the error space, of which there were 8^7 or 2,097,152.

The error space was analyzed to find if each point was local minima, and if so, in how many axes. The number of axes is referred to as the minima order. Figure 4 shows the percent of the inner points that were local minima in each of the minima orders. For clarity, points that were local minima in one axis were not counted again as local minima in two or more axes.

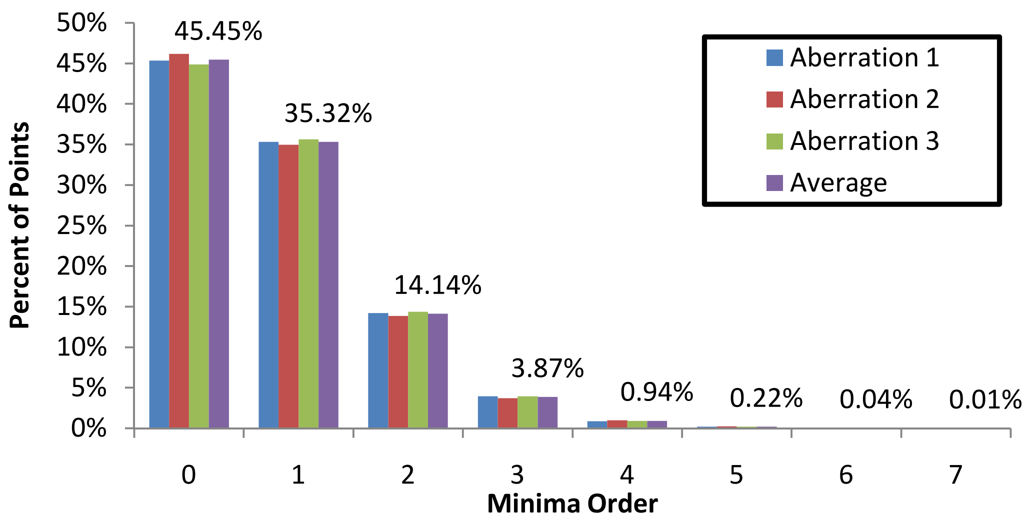

Figure 4 - Frequency of local minima with respect to the dimensionality of the minima for the three aberrations evaluated and their average.

We can learn quite a bit about the error space by analyzing this result. First, all the error spaces we analyzed were very similar statistically. In fact, the standard deviation of the percentages in any of the orders was always less than 1%. Although the majority of points were local minima in at least one axis, only 0.01% were fully-dimensional local minima. These are the local minima that are most difficult for simple searching algorithms.

3.2. Depth of Local Minima

Many searching algorithms have some degree of randomness built in to help them to hop out of local minima. We sought to determine the depth of the local minima to help determine how much randomness is necessary to avoid becoming trapped in a local minima. For this evaluation, we looked at all the local minima and determined the average depth by averaging the difference in metric value (Strehl ratio) between the local minima and all its neighbors in all the axes that were minima. We only looked at points on our grid of 10 points in each axis. Figure 5 shows the data plotted as a histogram to show how many of the minima were at what depth.

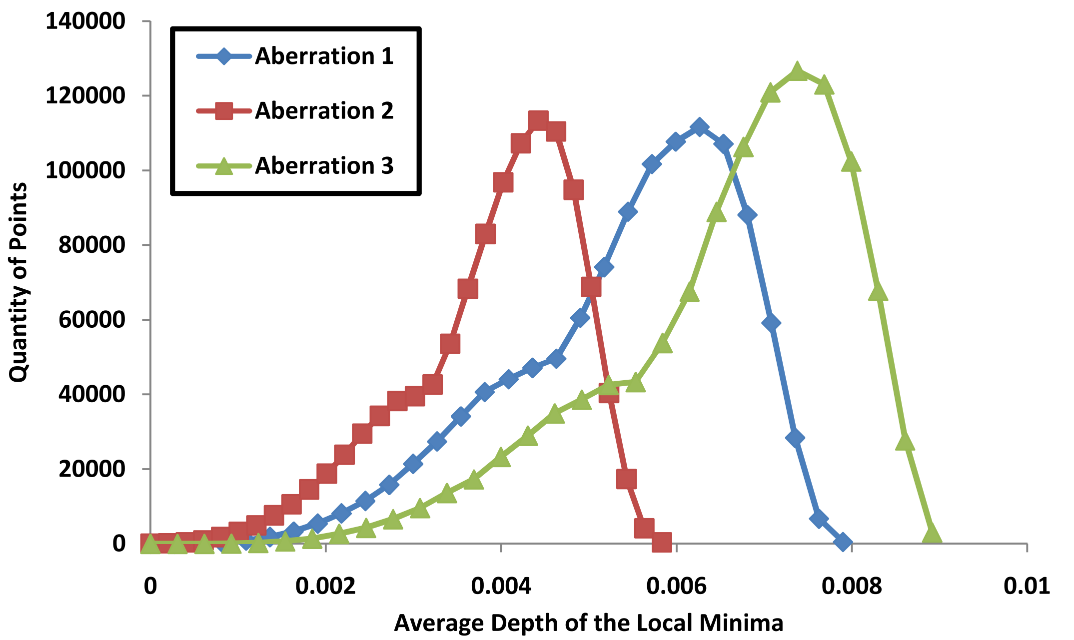

Figure 5 - Histogram of the depth of the local minima

From the data in Figure 5, we can see that in all the cases evaluated, the local minima have a very small depth and that most of the local minima are near the larger depths. The shape of the curves is clearly bimodal, but that is probably of less interest to general problems since it will probably be traced back to the specific model of the DM coupled with the specific merit function chosen. In all of our cases, the depth of the local minima were less than 0.01. Since these minima are at such a shallow depth, it is likely that measurement noise will enable the system to hop out of the local minima and sophisticated algorithms may not be necessary.

3.3. Location of Local Minima

So far we have found that there are very few fully-dimensional local minima and that they are quite shallow, but we have not looked at where these local minima are. To address that point, we looked at a histogram of the metric value (Strehl ratio) at each of the fully-dimensional local minima. Figure 6 shows this histogram of the value of all the fully-dimensional local minima for all of the error spaces we generated.

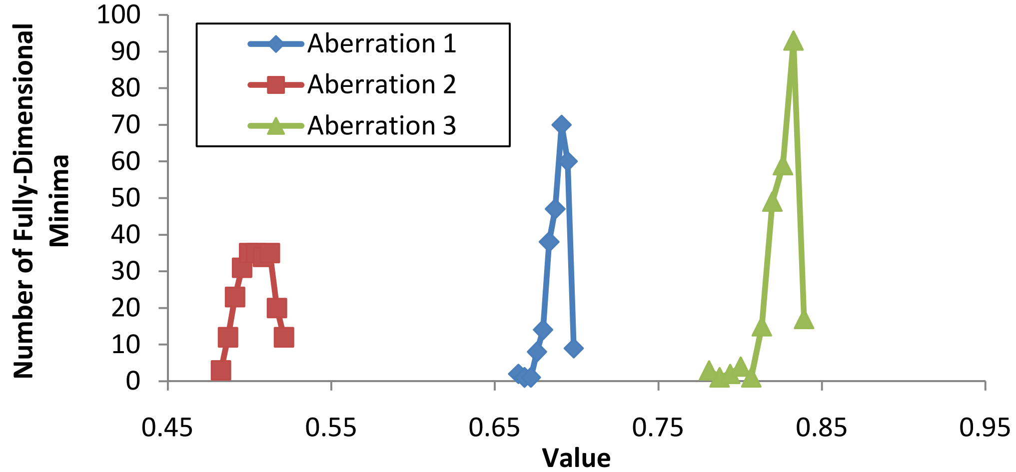

Figure 6 - Histograms of the fully-dimensional minima for each of the three aberrations

For comparison, Figure 7 shows the histogram of the all the data points we generated in the entire error space.

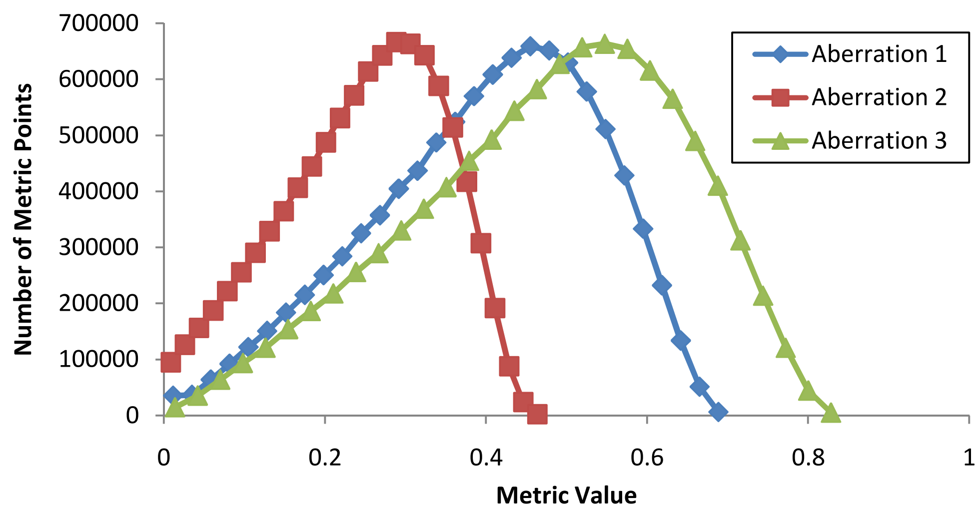

Figure 7 - Histogram of all the points in the metric error space

Table 1shows some of the statistics of the fully dimensional minima.

Table 1- Statistics of Fully Dimensional Local Minima

Aberration	1	2	3
Minimum	0.6626	0.4804	0.7778
Maximum (Optimum)	0.7002	0.5232	0.8424
Average	0.6885	0.5035	0.8263
StDev	0.0059	0.0094	0.0102
Count	250	240	244

This result was one of the most interesting of the study. In each of the three cases, the majority of the fully-dimensional local minima were very near the optimum value. In fact, the standard deviation of the fully-dimensional local minima was less than 1% in every case we examined. The range of values for the fully-dimensional local minima was less than 7% in every case as well. Thus, even if a searching algorithm were to get stuck in one of these local minima, we would be very near the optimum anyway.

3.4. Shape of the Error Space

Although visualizing these error spaces in more than a few dimensions is extremely difficult, we did want to show a limited dimensional visualization of the error space to give a flavor of the character of the space. Figure 8 shows a surface section of the error space near a fully-dimensional local minima. This plot shows that the error space is actually quite smooth. It also shows a common way that local minima occur. The local minima in this plot, which is indicated by the black asterisk, is actually on an angled ridge of minima.

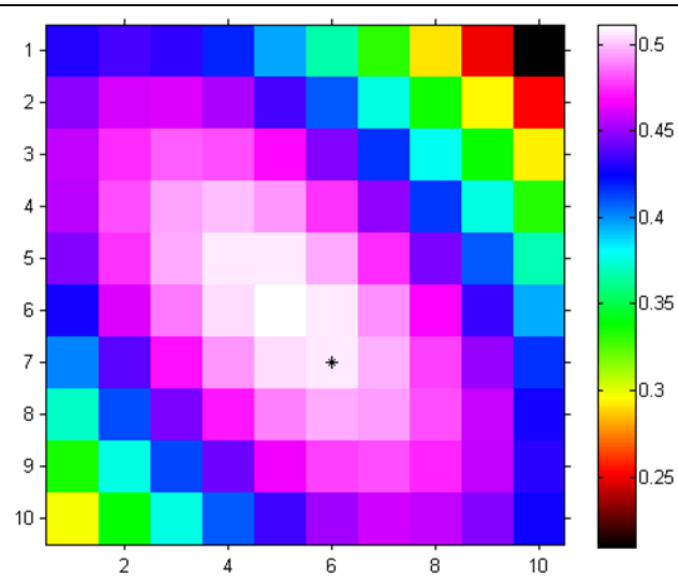

-0.5106	-0.5060	*-0.4908*
-0.5046	**-0.5061**	-0.4971
-0.4890	-0.4965	*-0.4935*

Figure 8 - Image of a section of the error space around a local minima. The local minima is indicated by the black asterisk. The values of the merit function around this local minima are shown in the table around the left

Examining the adjacent points show that it is indeed a local minima, but also shows that a point along the diagonal has a lower error, where error is the negative of the Strehl ratio. This type of local minima would fool many of the simple axial search algorithms, but would be easily avoided by more sophisticated algorithms.

4. CONCLUSIONS

Over the past several years we have seen some amazing results from metric adaptive optics systems. This study begins an analysis of the error space associated with typical metric AO systems and shows why local minima are not much of a problem for these AO systems. This study is just a single look at a few metric adaptive optics error spaces, but it is a common enough problem definition to be widely applicable. Future work on this topic may include a study of how different searching algorithms respond to traversing the error space and how the presence of these local minima affected their performance.

5. References

[1] J. Mansell et al., "Progress toward a Low-Cost Compact Adaptive Optics System", SPIE Vol. (2007).

[2] M. A. Vorontsov and G. W. Carhart, "Adaptive wavefront control with asynchronous stochastic parallel gradient descent clusters," J. Opt. Soc. Am. A **23**, 2613-2622 (2006).

[3] J. Mansell, "Micromachined deformable mirrors for laser wavefront control", Doctoral Dissertation at Stanford University, February 2002.

[4] M. J. Booth, "Wavefront sensorless adaptive optics for large aberrations," Opt. Lett. **32**, 5-7 (2007).